

A Review of End-of-Life Silicon Solar Photovoltaic Modules and the Potential for Electrochemical Recycling

Jackson Lee, Noel Duffy, and Jessica Allen*

The mass deployment of solar energy technology has been inspired by sustainable energy objectives. However, end-of-life solar photovoltaic modules present the growing dilemma of solar waste management. A circular economy approach should therefore be applied to the solar industry due to the valuable materials contained within modules, and their upfront emissions and energy intensity. Solar module recycling has to date been delineated into three phases: disassembly, delamination, and extraction. Disassembly has been commercially established; delamination has experienced some progression with further development required to liberate the valuable solar cell material, while extraction has had more limited exploration, predominantly through a hydrometallurgical lens. Extraction via electrochemical methods, however, has received some recent attention in the literature with promising outcomes for both metal extraction and process electrification. Electrochemical approaches offer new methods for more advanced processing options. For example, high-temperature molten salt electrorefining has been investigated for metallurgical-grade silicon and could prove to be an effective process for recovering silicon. This review provides an overview of solar module recovery methods, with focus on novel and emerging electrochemical approaches including the applicability of electrorefining to upgrade recovered silicon from photovoltaic waste.

1. Introduction

The world is currently undertaking a monumental transition away from fossil fuels under the threats of climate change, supply security, and worldwide depletion.^[1] To address the environmental and economic challenges, the global energy

system must undergo a clean energy revolution to replace greenhouse gas-emitting energy generators with sustainable energy producers.^[2] The two major resources that can be exploited for large-scale renewable energy deployment are wind and solar. Solar energy can be divided into photovoltaics (PV) and concentrated solar thermal energy. PV has been one of the fastest-growing energy technologies in the world since the early 21st century, with manufacturing methods experiencing increased effectiveness with reduced costs.^[1,3] In 2023, over 400 GW of new PV capacity was installed with China contributing 235 GW, America installing 33 GW, and the European Union adding 61 GW. This brought the cumulative worldwide capacity to 1,600 GW with further growth predicted to reach 4,500 GW by 2050.^[4]

With large-scale PV installation, there is a lagging issue of rising volumes of decommissioned end-of-life (EOL) solar modules.^[4b,5] The expected lifetime of a solar module is 25–30 years which can be used to predict the expected global mass

of EOL modules, however, it has been reported that ≈30% of decommissioned systems are less than 10 years old.^[5,6] PV waste is projected to be 8 million tonnes in 2030 and expected to cumulate 80 million tonnes by 2050. This would account for 10% of the global electronics waste by that time.^[5,7] The rising issue of PV waste couples an environmental challenge with a unique economic opportunity. The potential value of recoverable materials in cumulative EOL modules by 2050 has been estimated at \$15 billion US dollars (USD), with the capacity to produce 2 billion new modules equivalent to 630 GW of new capacity.^[4b,5] However, EOL modules are primarily disposed of in landfill due to the lack of cost effective recovery of high-purity materials in an environmentally conscious way.^[5,7,8]

The key components of PV modules are produced through energy-intensive refining processes which greatly contribute to the lifecycle emissions of the technology, which represents a significant amount of embodied carbon waste if disposed of in landfill.^[5,9] As a result, the successful rollout of an effective PV recycling process can reconcile the renewable energy transition with a circular economy, that minimizes waste and maximizes the recovery of high-value material such as high-purity silicon and silver while mitigating the depletion of critical resources.^[5]

J. Lee, J. Allen
Chemical Engineering
University of Newcastle
Callaghan, NSW 2308, Australia
E-mail: j.allen@newcastle.edu.au

N. Duffy
CSIRO Energy
Clayton, Victoria 3168, Australia

 The ORCID identification number(s) for the author(s) of this article can be found under <https://doi.org/10.1002/aesr.202400254>.

© 2024 The Author(s). Advanced Energy and Sustainability Research published by Wiley-VCH GmbH. This is an open access article under the terms of the Creative Commons Attribution License, which permits use, distribution and reproduction in any medium, provided the original work is properly cited.

DOI: [10.1002/aesr.202400254](https://doi.org/10.1002/aesr.202400254)

2. Global Approaches to EOL Management

2.1. Policy and Regulation

In the early 2000s, the European Union (EU) introduced the Waste Electrical and Electronic Equipment (WEEE) Directives to address the rising volumes of electronics waste in the 28 member states.^[10] In 2012, the regulation was expanded to include PV waste and assigned the main liability for the costs of collection, handling, and treatment to the manufacturers of PV modules.^[10a] The recovery targets were expanded by the EU in 2018 to 65% collection of equipment “put on the market” or 85% of waste generated, 85% of material recovery, and 80% recycled. Here, recovery is physical separation and reclamation of a specific material, while recycling is defined as the preparation of reclaimed material for treatment and reuse.^[4b]

The German government defined two financial mechanisms for PV recycling; Business-To-Consumer (B2C) and Business-To-Business (B2B).^[10a] The B2C model requires PV producers to collect and recycle any new household modules that enter the market, as well as any historic waste.^[4b,10a] The B2B model provides producers with two options in meeting their EOL obligations, either by contractual agreement or competitive market bids.^[4b,10a]

EU members have also adopted the WEEE directives in various ways such as in Italy which established a National Register to ensure producers are meeting compliance and obligations. Italy also collects a ‘feed-in’ tariff which is repaid to manufacturers if they can prove that PV modules were properly disposed of within six months of collection.^[10a] The Swedish government has also been proactive in managing PV waste through the SENS foundation which has collected over 70 tonnes of EOL modules since 2015.^[10a]

The UK adopted a similar model however, B2C financing is based on market share (e.g., if a producer introduces 10% of new modules in a given year they must finance the collection and recycling of 10% of EOL modules that year). In addition to this B2B required producers to exchange older modules that do not have compliant labeling with the WEEE Directives. The UK also requires producers to register for collection while in Germany registration is not mandatory and offers the flexibility to alternative financial models.^[10a]

Outside of Europe, the adoption of EOL PV legislation has been less comprehensive. The United States of America (USA) currently has no national PV-specific regulation,^[4b] however, some states have taken initiative in this area. In 2021, California reclassified PV modules from hazardous waste to universal waste, which subjects the stream to less stringent set of standards to ease the regulatory requirements to promote recycling.^[11] Washington passed a bill in 2017 which holds manufacturers accountable for their units and bans those without a recycling plan from selling modules in the Washington market as of 2021.^[10a] The Solar Energy Industries Association (SEIA), an industry group, also independently developed a proactive strategy to manage EOL solar waste. The basis of the strategy is to form a national recycling network with the goal of an international circular economy.^[10a]

Similar to the USA, Australia does not currently have a scheme or program for the collection, reuse or recycling of

decommissioned solar PV systems. However, in 2023, the Australian Government Department of Climate Change, Energy, the Environment and Water (DCCEEW) proposed a regulatory approach for electrical products which included PV modules. Similarly to the UK, this scheme would see liable parties paying fees proportionate to market share imported or produced annually. The scheme administrator would receive the funds which would cover the cost for collection, recycling, and reporting, and the financial lag would allow for the immediate access to funds to address legacy waste not covered by the scheme.^[12]

2.2. Industrial Scale Recycling

There has been a steady increase since 2017 in the number of recyclers that accept PV modules for the development and demonstration of recycling.^[13] While commercial recycling plants are in planning and construction stages, a complete comprehensive process with advanced treatment to separate high-quality materials is yet to be demonstrated. Furthermore publicly available data on these processes and their results are limited.^[13b] Five European (Reiling Glass Recycling, LuxChemtech, Flaxres, ROSI SAS, and Envie and Tialpi) and one United States (First Solar) companies leading the charge with pilot scale development with recycling capacities between 1 000 and 50 000 t year⁻¹.^[13b] Mechanical methods have traditionally been leveraged by these companies to optimize cost and capacity. This, however, down-grades material quality and limits what materials can be recovered. Whereas more innovative methods, while more limited by scale can separate and produce high-quality materials.^[13b] More broadly, there are over 50 solar panel recycling companies worldwide, the majority focusing on specific components and less than half have adopted a more comprehensive approach.^[13a]

3. Photovoltaic Technology

Silicon photovoltaics dominate the solar PV market and constitute over 90% of the global market.^[5,14] Despite developments made in alternative photovoltaic technologies, it is expected that silicon-based modules will continue to maintain market dominance up to 2030.^[4b] Due to the large projected market share and forecasted waste predictions of silicon photovoltaics, there is emphasis in research on the EOL management and recycling of these panels specifically.

3.1. Silicon Photovoltaics: Structure and Materials

The general design and structure of silicon photovoltaic panels are largely similar and can be represented as a number of layers. **Figure 1a** shows a diagrammatic representation of a solar panel with the layers separated in a deconstructed fashion; major layers in a panel include the backsheet, encapsulant, solar cells, glass, and frame.

3.1.1. Backsheet

The backsheet of a solar panel is often made from laminates of different polymers. It is common for these laminates to partly or

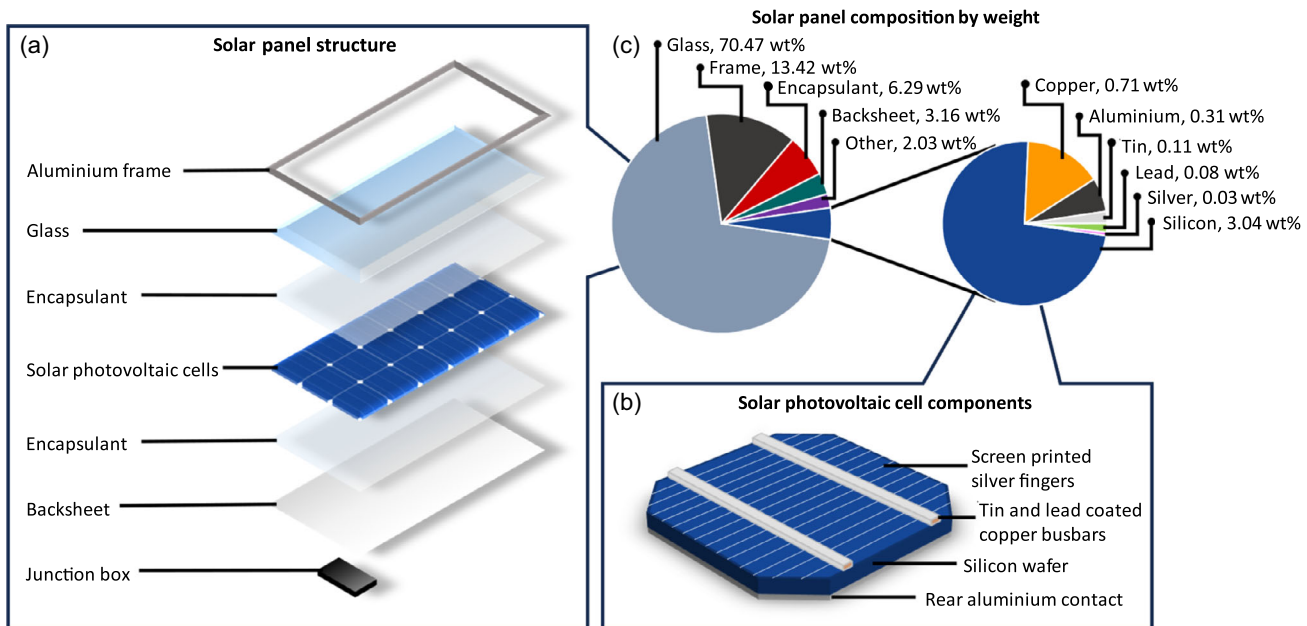


Figure 1. a) Deconstructed diagrammatic representation of a silicon solar panel structure; b) diagrammatic representation of a silicon solar photovoltaic cell composition; and c) silicon solar panel composition by weight, percentage. Produced from Table S1, Supporting Information using data from ref. [20].

entirely consist of fluorinated polymers such as polyvinyl fluoride (PVF), with Tedlar being the most commonly used material.^[15] Tedlar is a laminated polymer consisting of two layers of PVF with an internal layer of polyethylene terephthalate.^[16] Other backsheets may include polyvinylidene fluoride or ethylene chlorotrifluoroethylene.^[15b,17]

3.1.2. Encapsulant

The encapsulant used in crystalline silicon modules is generally ethylene vinyl acetate (EVA). The EVA is used to adhere the backsheet, solar cells, and glass layers of the module together. The encapsulant is also used as a sealant to protect the module from thermal, mechanical, ultraviolet, and moisture attacks.^[15]

3.1.3. Solar Cells

The solar cells are responsible for generating power via the photovoltaic effect and is diagrammatically represented in Figure 1b.^[15b,18] Photovoltaic cells are composed of a silicon wafer and three metallic current collectors; silver, aluminum, and copper. Currently, silicon wafers are generally 180 to 200 μm thick and are either p-type or n-type.^[5,15b,18] P-type and n-type wafers are generally doped with either boron or phosphorous respectively.^[18] To form the n-p junction, a counter polarity dopant (e.g., phosphorous for p-type wafers or boron for n-type wafers) is diffused onto the top surface of the wafer. The surface is then textured and coated with an antireflecting coating (ARC).^[18] Common ARCs include silicon nitride (Si_3N_4), titanium dioxide (TiO_2), silicon monoxide (SiO), silicon dioxide (SiO_2), and aluminum oxide (Al_2O_3).^[15b,19]

On the top surface are screen printed silver fingers and a full area aluminum coating on the rear. Individual cells are connected in series using copper busbars or ribbons that run perpendicular to the silver fingers.^[18,20c] The busbars that connect the cells consist of a copper core coated in tin and are generally attached using lead solder. However, the PV manufacturing industry is making progress to move away from the utilization of lead.^[15b,20c] The busbars deliver the current to the junction box on the back of the panel. These junction boxes contain diodes and cables which connect panels together in a PV system.^[14,20c]

3.1.4. Glass and External Frame

Tempered, low iron glass is used on the front of solar panels.^[15b,21] The glass is highly shock resistant to protect the solar cells and highly transparent allowing light to pass through. The glass layer provides structure and security for the cells from the external elements to prevent internal damage.^[15a,18] The aluminum-based external frame helps hold the panel together and protects the internal layers as they are sealed in with silicone rubber.^[15]

3.2. The Need for a Circular Solar Economy

Waste modules can be considered a rich source of valuable materials such as silicon, silver, copper, aluminum, and glass.^[5,20b] Figure 1c compares compositional breakdowns of crystalline silicon solar panels reported in the literature, a more in-depth comparison can be seen in Table S1, Supporting Information. It can be observed that on average the solar glass accounts for majority of the weight of the panel at $\approx 70\%$ and the aluminum frame making up roughly 14%. Additionally, the photovoltaic cells

contribute over 4% to the weight of the panel. As a result, each tonne of module waste contains \approx 137 kg of aluminum, 30 kg of high-purity silicon, 7 kg of copper, and 300 g of silver. This content is comparable to the declining state of ore grades. The current average global copper content in mined ore is \approx 7 kg per tonne, and the silver content in mined copper ores was reported at 300 g per tonne.^[22] Therefore, the recovery of valuable materials from photovoltaic waste can be considered as a new generation of sustainable mining that keeps valuable materials in circulation, mitigating material depletion.^[20b] However, the most valuable components of waste solar panels are the materials in the photovoltaic cells and busbars which include silver, copper, and silicon. The reported market price of silver ranges from \$440 to \$740 USD per kilogram, copper ranges between \$4.4 and \$11 USD per kilogram, and the price of metallurgical-grade silicon is between \$1.7 and \$2.7 USD per kilogram.^[20b,20c,20e] As a result, the potential value from these three materials is between \$210 and \$380 USD per tonne of waste solar panels, not accounting for the cost of recycling. Including the value of the recyclable aluminum frame with a market value of \$1–\$2 USD per kilogram^[20c] the value increases to \$350–\$654 USD per tonne. Figure 2 shows a comparison of the metal content in copper ore and EOL solar modules as well as the potential value of the materials per tonne. This further illustrates that solar module recycling is equivalent to current ore grades. However, when the high mass content material of solar modules (such as aluminum frame and solar glass) is removed the concentration of silver and copper increases whereas ore grades are predicted to continue to decline.^[22b]

For crystalline silicon modules, the biggest environmental impact is due to the large electrical and chemical energy consumption required to produce the high-purity silicon. The emission intensity varies on the energy mix powering the process, which is largely fossil fuel based.^[23] As a result, over a 30 years lifetime, PV systems can have an emissions factor of 13 to 104 g

of CO₂ equivalent per kilowatt hour, with approximately half the embodied energy and climate change impact just from the silicon wafer.^[5,9a] There is also the financial incentive to recover high-grade silicon as it increases the value when compared to metallurgical silicon to \$10 USD per kilogram.^[5]

Moreover, PV modules contain hazardous substances such as lead and silver that can have serious environmental consequences if released. Modules placed in municipal wastes streams can leach substances into the environment and cause acute toxicity in wildlife, as well as water and soil pollution.^[24] A study conducted by Nain and Kumar^[25] investigated heavy metals leaching out of solar modules over a year. They investigated various modules with different pH solutions as well as a municipal waste leachate from Okhla landfill in India. It was found that the encapsulant degradation is strongly coupled with metal leaching. More than 30 mg L⁻¹ of lead was observed to leach from broken PV modules over the course of a year, increasing the probability of exceeding surface water limits by 90% and doubling the contamination potential of a disposal site.^[25]

4. Approaches to Photovoltaic Module Recycling

The current approaches to deconstructing a photovoltaic module back into its raw materials have three distinct phases. Phase one is the disassembly of the aluminum frame and junction box. The second phase is the delamination of the layered structure coupled with material sorting processes and is considered the most complex phase due to processing challenges such as pollution and cost. The third phase then involves material extraction. This phase focuses on the recovery of valuable materials in a way that they can be reclaimed for reuse in the supply chain.^[20b,20d] Each phase can be made of multiple processes and operations with different techniques and methods explored such as mechanical, thermal, and chemical.^[15b,20b,20d]

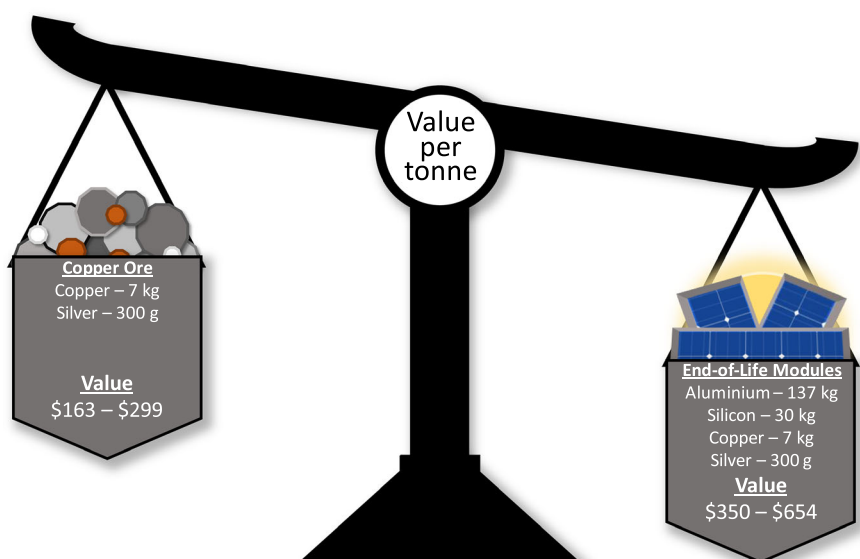


Figure 2. Comparison of metal content in copper ore and end-of-life solar modules and the estimated value per tonne based on data from Figure 1 and refs. [20b,20c,20e,22,60].

4.1. Phase One: Disassembly

Module disassembly consists of the removal of the aluminum frame, junction boxes, and cables as pictured in **Figure 3**, and also produces a laminate structure of the solar glass, encapsulant, solar cells, and backsheets.

The cables and junction boxes are generally removed first which can be processed at an e-waste recycling facility to recover the copper and repurpose other materials.^[15b,26] The main part of module disassembly is the removal of the aluminum frame which unlocks the laminate structure to allow for delamination. This is a process that uses mechanical force to remove the module frame.^[15,20,27] Additionally, there is a large demand as well as an established market for recycled

aluminum, with an economic benefit of $\approx \$1\text{--}2$ USD per kilogram.^[20b]

4.2. Phase Two: Delamination

Delamination methods are classified as mechanical, thermal, or chemical. The method of choice varies based on the target material and specific process steps chosen. The objective, however, remains the same; layer separation and encapsulant removal allowing for the recovery of high-grade solar glass, silicon wafers, and valuable metals as raw materials for reuse.^[15b,20b] **Figure 4** schematically shows the delamination of the glass, photovoltaic cells, and backsheets from the encapsulant.

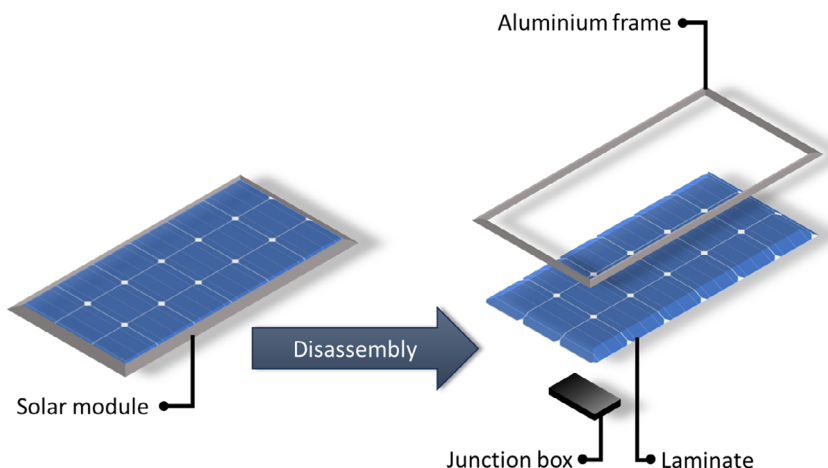


Figure 3. Phase one—disassembly of junction box and aluminum frame, leaving a laminate of glass, EVA (top layer), solar cells, EVA (bottom layer), and backsheets.

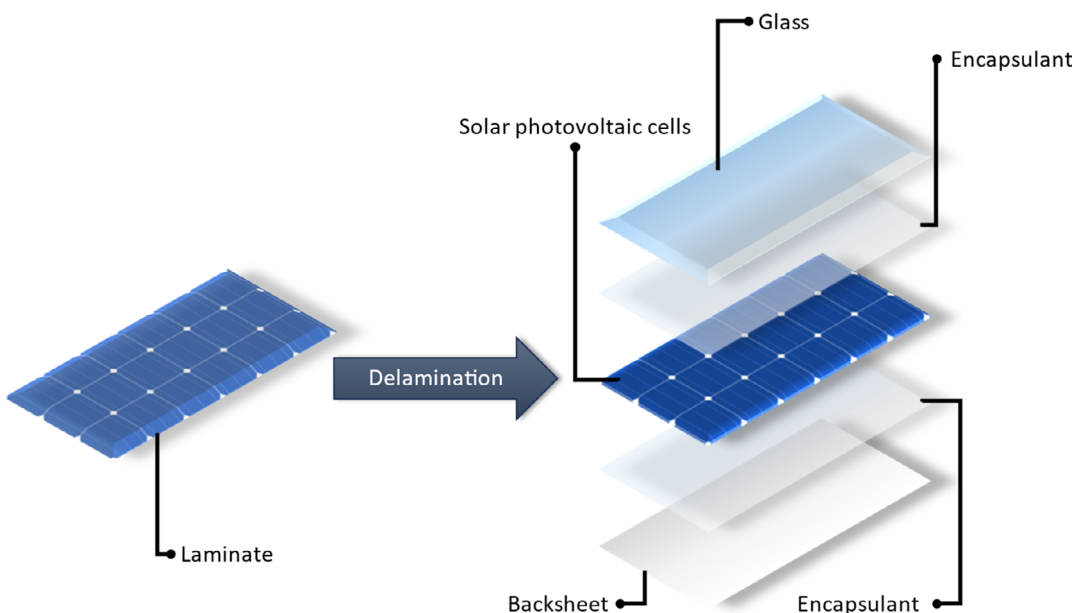


Figure 4. Phase two—delamination of the glass, solar photovoltaic cells, and backsheets from the EVA encapsulant.

4.2.1. Mechanical Delamination

A variety of mechanical approaches have been explored in the literature targeting either a broad range of materials or highly selective layer removal. Dias et al.^[27] investigated the potential of milling deframed panels and using electrostatic separation to segregate the conductive from non-conductive material. It was found by Dias et al.^[26] that electrostatic separation was able to concentrate the metallic fraction to $\approx 95\%$ in the recombined conductive and middling fractions. However, it was unable to concentrate polymers and the glass tended to accumulate in the conductive fraction. Of the variables tested, they were unable to determine optimal operating conditions to separate metals from polymers.^[28] de Souza et al.^[28] continued the work of electrostatic separation and found that the ideal conditions were a potential difference of 38 kV with a rotation speed of 75 rpm. Additionally, the separation efficiency between conductive and no-conductive fractions was high with 88% being the best efficiency rate obtained for silver. However, de Souza et al.^[28] mainly focused on the optimal operating conditions to achieve the highest concentration of conductive metals and did not investigate how these conditions affect the polymers and glass included in the feed.

The hot knife method has undergone development by NPC incorporated in Japan and is an automated disassembly line that facilitates the removal of the junction box, aluminum frame, and glass separation.^[29] The process utilizes a heated cutter (180 to 200 °C) to separate the glass from the laminate at a rate of 50 s per module. Alternatively, Fiandra et al.^[30] investigated the selective removal of the backsheet using a milling machine. For a panel with the dimensions of 100 cm by 45 cm, the milling process took 8 min and produced encapsulant/backsheet chips. While this method is more novel than the hot knife method, it does share some similar limitations such as single-panel processing and the requirement of flat, unbent panels. It also has a much longer processing time and is more sensitive to changes in panel design to ensure complete backsheet removal without damage to the underlying cells and glass.^[30]

From the mechanical methods reviewed, there are two approaches in development, bulk commercial delamination and single-panel processing methods. The bulk processes can handle a much larger throughput on a commercial scale but have a low material selectivity due to cross-contamination in material separation. Meanwhile, the single-panel processing methods have a high selectivity and can output products with a comparatively low level of contamination, at the expense of processing time and sensitivity to module design and physical condition.

4.2.2. Thermal Delamination

Thermal delamination methods are centered around the thermal degradation of the polymeric materials in the panels and have often been performed in the literature in a two-step process. The first step consists of the physical removal of the backsheet and the second step is the thermal treatment. The main reason for backsheet removal is due to the fluorine content, which produces fluorinated byproducts during heat treatment.^[15b] In addition to the generation of hazardous pollutants, the process is

highly energy intensive and results in the loss of the polymeric materials which can no longer be repurposed.^[15b,31]

Fiandra et al.^[30] employed thermal delamination after the removal of the backsheet via milling. This was performed in a tube furnace at 450, 500, and 600 °C with a heating rate of 7.5 °C per minute and dwell time for 1 h. It was found that the optimal operating conditions were achieved at 500 °C with an oxidizing atmosphere. This is due to a lower production rate of volatile organic compounds as the partially degraded products were further oxidized to carbon dioxide. Additionally, no benzene or carbon chains greater than 5 carbon atoms long were formed unlike the products detected when performed in an inert atmosphere.^[30]

Wang et al.^[32] investigated the thermal delamination of crystalline silicon photovoltaics under pyrolysis conditions. Laminates were heated to 500 °C in a tube furnace under nitrogen for 1 h. It was found that the encapsulant can be completely removed above 450 °C, while below 450 °C a dark-colored viscous solid was observed on the remaining product. Wang et al.^[32] also detected the presence of volatile organic compounds, notably benzene, and compounds with carbon chains longer than 5 carbon atoms in agreement with Fiandra et al.^[30] results under an inert atmosphere. Both Wang et al.^[32] and Fiandra et al.^[30] described the thermal decomposition of EVA in two stages. The first stage eliminates the acetic acid via a deacetylation reaction which occurs between 300 and 400 °C. The second stage is the decomposition of the carbon backbone above 410 °C, which leads to the evolution of the volatile organic compounds with the final composition depending on the gas atmosphere used.

4.2.3. Chemical Delamination

The chemical delamination approach utilizes a solvent to penetrate the encapsulant and swell it into a gel-like polymer followed by the physical liberation of the valuable materials.^[15b,33] However, this method gives rise to certain challenges that must be overcome. These difficulties include the shattering of silicon wafers, toxic nature of the conventional solvents, and long reaction times.^[15b] The breakage of silicon wafers is only an issue if the desired outcome is the recovery of whole wafers which is advised against by Heath et al.^[5] as the industry is unlikely to be interested in outdated wafers due to increasing cell efficiencies, changing cell technologies and chemistries, and wafers are often broken at EOL. As such, the research focus in chemical delamination has prioritized alternative solvents over those currently used which can be harmful and are fossil fuel derived.^[15b,31b]

Organic solvents were first proposed by Doi et al.^[34] as a method of chemical delamination. In their investigations, they screened a variety of organic solvents on non-cross-linked and cross-linked EVA. Some of the solvents tested include acetone, toluene, ethanol, isopropanol, and trichloroethylene. Most of the solvents analyzed could dissolve the EVA before cross-linking (which occurs during the encapsulation process) and fewer could only swell the cross-linked EVA. The more favorable results were achieved with trichloroethylene at 80 °C. Doi et al.^[34] then tested the separation effectiveness of trichloroethylene on prepared “one cell” modules with a structure of glass/EVA/PV cell/

EVA/aluminum foil. From these tests, they proposed a three-step mechanism for the delamination process. The first step is the increase of EVA fluidity as the temperature is increased, followed by the outward flow of non-cross-linked EVA by dissolution, and then the swelling of the cross-linked component. It was also observed that mechanical pressure applies a force perpendicular to the direction of swelling which leads to the cracking of PV cells.^[34]

Chitra et al.^[31b] recently continued this work and investigated the use of organic solvents to recover the polymeric layers from waste solar modules. In their work, they characterized the swelling properties of six organic solvents on a commercial EVA sheet. Of the solvents tested at room temperature, acetone, cyclohexane, and methanol had no reaction over 18 h. Chloroform and trichloroethylene swelled the EVA in 15 min, dissolved it after an hour, and dissolution was observed with toluene after 30 min. Chitra et al.^[31b] selected toluene to investigate the potential recovery of polymeric layers due to a lower volatility and toxicity when compared to the other organic solvents, highlighting the need for safer alternatives. The toluene at room temperature over 3 days was able to separate the layers of a small (0.13 m by 0.20 m) discarded polycrystalline photovoltaic module and allowed for the collection of EVA in a gel-like form via filtration.^[31b]

Brenes et al.^[35] aimed to improve the chemical process. They compared the effect of hexane, benzene, and toluene on EVA. Hexane was found to have no effect, benzene was able to form a gel with the EVA at 70 °C after 30 min and toluene was able to show signs of separation after 15 min at 70 °C. It was also found by employing calcination that the residual EVA on the solar cells after the chemical treatment with toluene was ≈16%.^[35] It is generally agreed in the literature that toluene is one of the most effective and safest of the organic solvents in terms of solar module delamination. However, it still poses health and environmental hazards and safer alternatives would be industrially preferred.^[15b]

An alternative solvent to toluene that has recently been explored in the literature is d-limonene, a bio-based solvent.^[31a,36] Abdo et al.^[31a] investigated the use of d-limonene to delaminate the backsheet and found that the solvent could achieve 100% backsheet delamination at 60 °C in 120 min under ultrasonication (450 W). It was also found that the solvent could continue to achieve 100% backsheet removal when reused for three cycles.^[31a] However, this work did not quantify the separation beyond backsheet removal (did not investigate the separation of solar cell material, glass, and EVA), or directly compare the performance of d-limonene to toluene. Lee et al.^[36] continued this work and quantified the solar cell material liberation from photovoltaic laminates using both toluene and d-limonene. It was determined that d-limonene can liberate up to 4.5 times more solar cell material than toluene while maintaining a similar degree of separation.^[36] The work done by Lee et al.^[36] also highlights the different observations reported in chemical separation methods where some works report swelling,^[35,36] while others report a more complete dissolution and separation.^[31b] It is theorized based on the proposed mechanism by Doi et al.^[34] that this is due to the different modules used in experimentation, with commercial modules manufactured with a higher degree of EVA cross-linking and the smaller polycrystalline module having a lesser degree of cross-linking.^[36] Therefore, chemical

separation methods can be sensitive to differences in manufacturing, however, recycling necessitates independence from such variable factors.

4.2.4. Material Sorting

Materials sorting processes are generally coupled with delamination, much like the case of electrostatic separation after a mechanical shredding process.^[15b,20b] Electrostatic separation is based on the differences of the electrostatic characteristics, while other sorting processes are based on different material properties such as particle size, density, and optical transmittance.^[20b,28] Deng et al.^[20b] outlines three other common materials sorting processes in literature which are vibratory screens, density separation, and optical sorting and can be schematically seen in Figure 5.^[20b]

Vibrating screens separate different fractions based on particle size after an attrition process. The larger particles (generally sized greater than 5.0 mm) consist of polymers and copper ribbons. These materials are more elastic and flexible than other components and as a result, are less likely to fragment due to size reduction. However, due to the encapsulant there is contamination of glass, silicon, and silver in the larger fraction. This is due to size reduction not completely separating the materials and completely delaminating the structure. The lower fractions (less than 5 mm) generally consist of glass.^[20b] These results are based on materials sorting after mechanical size reduction and would differ completely if this separation was used to sort materials that have been thermally or chemically separated. Optical sorting has been used by at least three different solar panel recycling facilities in Europe such as the Italian startup Tialpi Srl.^[20b,37] The technology utilizes an optical sensor to analyze the color of module fragments and uses an ejector (generally compressed air) to sort the size-reduced module components.^[20b] This method is limited to sorting based purely on color and misread measurements are heavily influenced by complex shapes, illumination variation, and distance changes.^[38]

Density separation utilizes a fluid of intermediate density to float the materials less dense than the fluid, and sink those that are more dense.^[20b] Akimoto et al.^[39] was able to concentrate silicon and silver from glass and other contaminants using sodium polytungstate as a dense medium. Alternatively, Dhawan et al.^[40] investigated the use of fluidizing water to enrich silver and silicon prior to hydrometallurgical techniques. The used solar panels were de-framed, de-glassed, milled, and sieved into three fraction; greater than 100, 100–53 µm, and less than 53 µm. The two larger fractions underwent fluidization. The fraction greater than 100 µm had a metallic recovery of 98.5 wt% in the underflow with an EVA contamination of 4.5 wt%, while the 100–53 µm had a metallic recovery of 96.1 wt% in the underflow with an EVA presence of 13.3 wt%.^[40]

4.3. Phase Three: Material Extraction

4.3.1. Hydrometallurgical Extraction

Once the solar modules have been disassembled and delaminated, the valuable materials in the solar photovoltaic cells

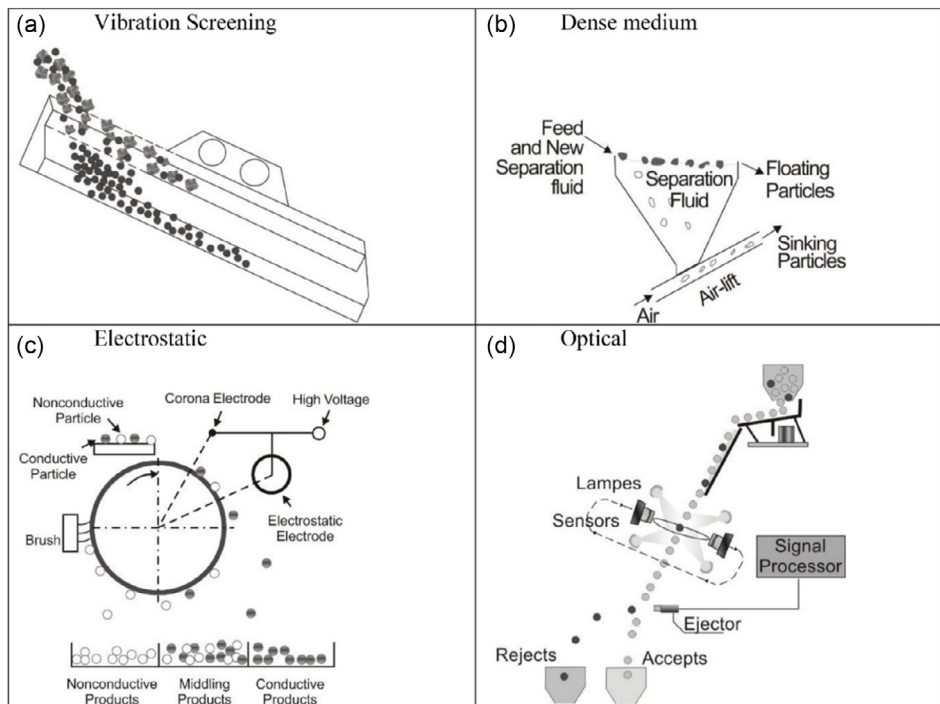


Figure 5. Schematics of mainstream material separation technologies: a) vibration screening, b) density separation, c) electrostatic separation, and d) optical sorting. Reproduced with permission.^[16b] Copyright 2022, Elsevier.

(silicon, silver, and copper) can then be extracted and recovered. Figure 6 diagrammatically shows the separation of the rear aluminum contact as well as the surface metals (e.g., silver and copper) from the silicon material in an extractable form.

For metal recovery, there are two different practices explored in the literature, hydrometallurgy and electrochemical methods. Gahlot et al.^[20e] outlined that hydrometallurgy is commonly leveraged in the literature due to the metal content and different solubility parameters of the metallic components, despite the large chemical requirement and wastewater generation. The research focus and applied method vary dependent on the targeted material, leachates used, and desired product form.

Klugmann-Radziemska et al.^[19] used a three-step selective chemical etching process to recover the underlying silicon

material. The first step removed the rear aluminum contact via a 30 wt% solution of potassium hydroxide (KOH) at 80 °C for 3 min. The second step removed the silver using a 40% nitric acid (HNO₃) solution at 80 °C for 15 min. Once the non-silicon metals were removed Klugmann-Radziemska et al.^[19] aimed to recover the base silicon metal which involved the removal of the anti-reflective coating and n-p junction. This was achieved using a solution of 29.4 wt% HNO₃, 10.8 wt% hydrofluoric acid (HF), 27.0 wt% acetic acid (CH₃COOH), and 0.5 wt% bromine. As a result of chemical etching, the overall thickness of the silicon decreased by ≈20 µm. It was also found that the solution had to be modified for different cells tested, despite an aim to develop a universal etching solution. This process also involves the use of HF and the generation of nitric oxides, which are industrially

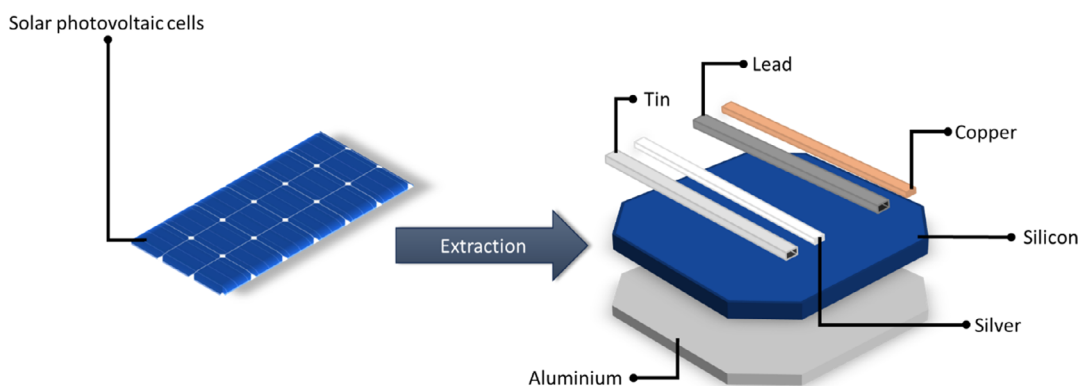


Figure 6. Phase three—extraction of valuable materials from the solar cells for recovery and reuse.

expensive both operationally (highly hazardous) and in terms of disposal. Furthermore, this is a parasitic process and leads to an overall silicon loss.^[19]

Similarly, Kang et al.^[41] used a combination of HF, HNO₃, and CH₃COOH to leach the metals and etch away the antireflective coating from photovoltaic cells recovered from modules. Kang et al.^[41] explains HF is necessary when decomposing silicates, HNO₃ is an oxidizing agent which can dissolve silver and other metals while CH₃COOH was added to improve the rate of dissolution. This successfully removed the metal impurities after 20 min. However, the etching solution also removed silicon, and the yield was severely impacted. Kang et al.^[41] also tested the addition of the surfactant CMP-MO-2 to the solution. The optimal concentration of the surfactant was found to be 20 wt% of the solution which increased silicon yield from 79 to 87 wt%. Kang et al.^[41] theorized that the increased yield was due to the formation of micelles at the surface of the cell, obstructing the contact between the etching solution and silicon. The final purity of the recovered silicon obtained was 99.999%.^[41] Riech et al.^[42] also investigated the usage of a HF and HNO₃ solution to recover silicon from EOL solar modules. Recovered solar cells from EOL modules were treated with an acid solution of 63.6 wt% HNO₃ and 3.6 wt% HF. After the chemical treatment with the acid solution 90 wt% of the silicon was recovered regardless of exposure time, and after 24 h the blue color on the silicon had completely disappeared implying the removal of the anti-reflective coating. This is in opposition to the findings of Kang et al.^[41] suggesting that the addition of CH₃COOH greatly impacts the etching behavior of the solution. However, the final purity of the silicon was not analyzed so the final product cannot be compared to the works of Kang et al.^[41]

To understand the impact of hydrofluoric acid, Prasad et al.^[43] compared the use of alkali chemical treatment with and without HF. Two solutions of 15 wt% sodium hydroxide (NaOH) and 15 wt% KOH were compared in a 15 min treatment. It was found that the NaOH solution had a marginal improvement in impurity removal from the silicon but was significantly more cost effective than the KOH. Based on the lower cost being more commercially attractive, the NaOH solution was then compared to HF. The NaOH treatment had a smaller weight loss and comparable impurity reduction to HF. However, the HF was able to successfully remove the anti-reflective coating, whereas the alkaline solution could not. Moreover, it was determined that HF has a rapid silicon etch rate which must be carefully accounted for to prevent the loss of silicon, which shows agreement with Klugmann-Radziemska et al.^[19] and Kang et al.^[41] but seemingly contradicts the observation made by Riech et al.^[42] that silicon recovery was constant regardless of exposure time.

Yi et al.^[44] investigated alternative leachates such as hydrochloric acid (HCl), sulfuric acid (H₂SO₄), HNO₃, and NaOH to remove the metals (silver, aluminum, and copper) from the silicon. Then attempts were made to purify the silicon through pyrometallurgical means. It was found that both HCl and H₂SO₄ were ineffective for silver dissolution due to the formation of the insoluble salts silver chloride and silver sulfate respectively. Additionally, aluminum could only be fully dissolved in NaOH after being treated with HNO₃. This process produced a silicon product with a purity of 99.98%. The resultant silicon was also compliant with the 5 N Symphony Silicon Ltd.

specification for phosphorous and boron (<5 and <3 mg kg⁻¹ respectively), but the total metal content was still above the specification of <2 mg kg⁻¹.^[44] The chemically treated silicon was smelted with a slag mixture of CaO, CaF, and SiO₂ at 1,520 °C for 6 h. The ideal results were obtained when a slag-to-silicon ratio of 7:1 was used which yielded a silicon purity of >99.998%. The smelting process also generated fluoride gases with silver, sodium, aluminum, and silicon which implies the commercial use of this process would require gas emission treatment.^[44]

Theocharis et al.^[45] proposed an integrated hydrometallurgical approach to recover pure silicon and silver from EOL solar modules. Figure 7^[45] shows an outline of the proposed process.

Figure 7 starts with a thermal treatment at 500 °C for 15 min in air to eliminate the polymeric materials. Sieving is then used to separate the glass from the remaining material. After which the photovoltaic material is ground in a ball mill. The photovoltaic powder below 90 µm undergoes the first leaching step in 6.0 M H₂SO₄ at 25 °C with a solid-to-liquid ratio of 5 wt%. This dissolves the rear aluminum contact, which can then be recovered after the solids are filtered off by the addition of 5.0 M NaOH. This precipitates the aluminum in the form of aluminum hydroxide and neutralizes the effluent solution. The solids after the first leaching step then undergo secondary leaching with 5 M HNO₃ at 25 °C with a solids to liquids ratio of 30 wt%. This step removes all the remaining metals (silver, copper, and lead) from the silicon wafer into solution. The silicon wafer then undergoes etching in 2.5 M NaOH at 25 °C to remove the antireflective coating. The metals that were leached via the nitric acid can then be recovered metallurgically or electrochemically. The metallurgical route involves the precipitation of silver chloride (AgCl) via the addition of hydrochloric acid or sodium chloride. The solution is then neutralized with 5.0 M NaOH which allows for the recovery of copper and lead hydroxides.^[45] Theocharis et al.^[45] found the first leaching step necessary by selectively leaching the aluminum which avoided the simultaneous dissolution of aluminum and silver in nitric acid. Silver extraction did not occur in the sulfuric acid at any concentration tested unless hydrogen peroxide was added. The nitric acid leaching was able to leach out the silver as well as copper, lead, and aluminum at room temperature. This also shows that aluminum will be leached out in the nitric acid if not removed prior.

5. Electrochemical Extraction

Alternatively to hydrometallurgical methods, leached metals can be directly extracted via electrochemical means. Sequential electrowinning is based on the different reduction potentials of the metals present in solution.^[45,46] Table 1 lists the standard reduction potentials for common metals used in photovoltaic cells.^[47]

This electrochemical sequence shows that silver can theoretically be extracted first from the application of an appropriate potential, then followed by copper, lead, and aluminum through increasingly negative potentials with no overlaps.^[46]

Theocharis et al.^[45] also investigated the possibility of electrowinning the silver out of the solution which can also be seen in Figure 7. This was tested by leaching powdered PV samples in 3 M nitric acid with a solids-to-liquids ratio of 30 wt% for 4 h. To

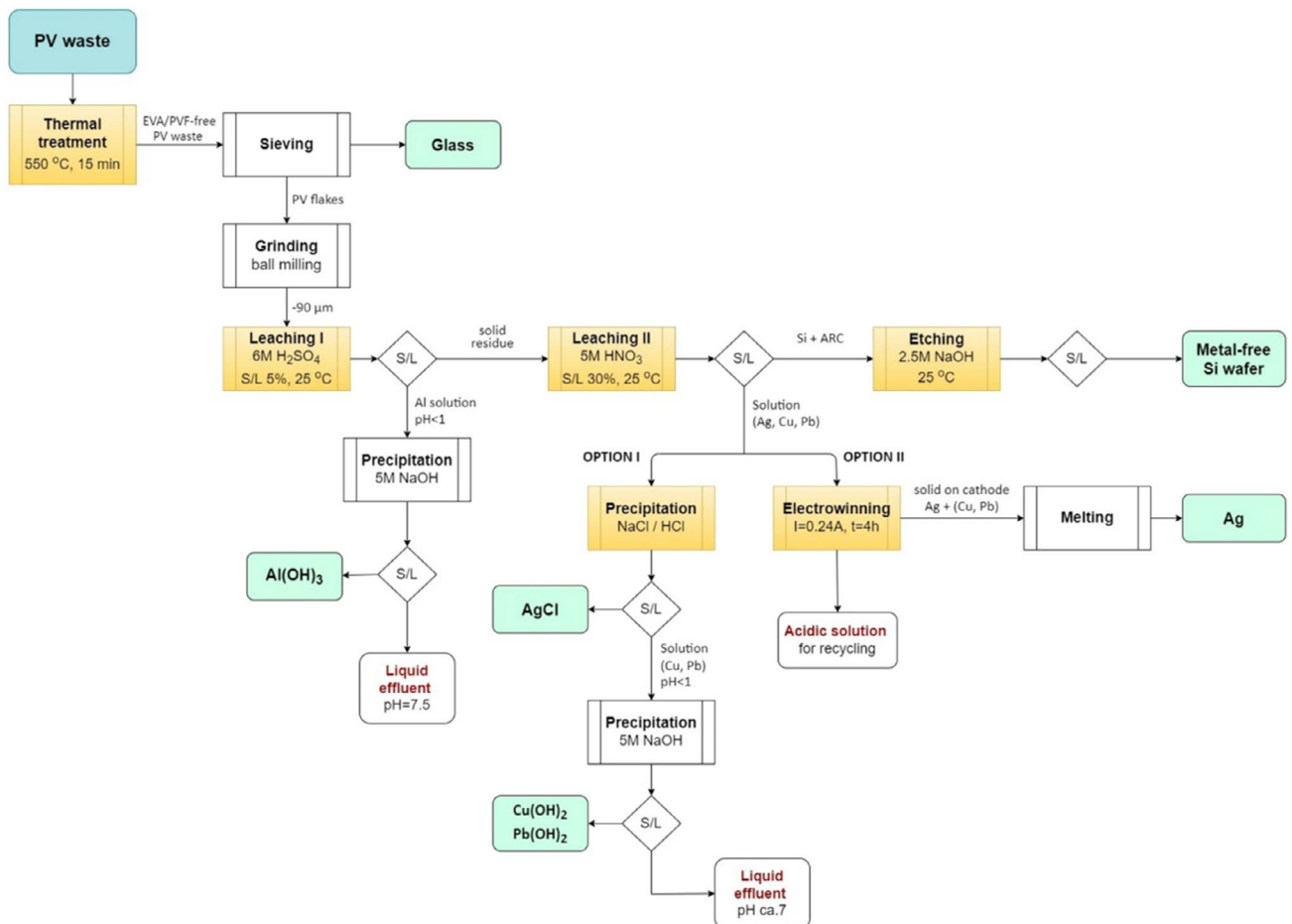


Figure 7. Process flowsheet for two-step extraction with H_2SO_4 and HNO_3 . Reproduced with permission.^[45] Copyright 2022, Springer Nature.

Table 1. Standard reduction potentials of common metals used in photovoltaic cells.^[47]

Electrochemical reaction	Literature standard reduction potential, E^0 (V)
$\text{Ag}^+ + e^- \rightarrow \text{Ag}_{(s)}$	0.799
$\text{Cu}^{2+} + 2e^- \rightarrow \text{Cu}_{(s)}$	0.337
$\text{Pb}^{2+} + 2e^- \rightarrow \text{Pb}_{(s)}$	-0.126
$\text{Al}^{3+} + 3e^- \rightarrow \text{Al}_{(s)}$	-1.660

electrowin in the silver, a two-electrode system was used with a titanium plate cathode with effective surface area of 1.0 cm^2 and a carbon rod or platinum plate anode with a surface area of 625.0 mm^2 . The system was held at a current of 0.24 A and potential varied between 3 and 5 V over the course of 10 h . For both PV samples tested, 100% silver removal was achieved after 4 to 5 h . It was found that in the highly acidic solution, the material formed on the cathode also favored the formation of aluminum and lead hydrolysis products, which presented as impurities in the metallic silver collected on the cathode. Copper was also found in the cathode deposit as it was simultaneously reduced with silver, no

doubt a result of poor voltage control. Theocharis et al.^[45] also recommends that aluminum should be removed in a separate step especially if electrowinning is to be used to recover the silver. Alternatively, voltage control rather than current control should be considered to ensure no overlap of deposition voltages.

Metallurgical and electrochemical methods do not have to be mutually exclusive and can be used in conjunction with each other. This was the approach taken by Jung et al.^[48] This method used manual and thermal methods to recover the photovoltaic cell material from modules. This material was leached in 5 M HNO_3 at room temperature to dissolve the copper, silver, and lead. To isolate the copper ions from the HNO_3 solution into a H_2SO_4 solution, solvent extraction was employed. A two-electrode system was used to deposit copper metal onto a copper plate cathode using a titanium plate with iridium oxide anode. A current density of 5 mA cm^{-2} was applied for 24 h at 50°C and the distance between the electrodes was 11.5 cm . This resulted in a copper recovery rate of 79 wt\% .^[48] It was also observed that the reaction increased the H_2SO_4 concentration as a result of the decreasing Cu^{2+} concentration implying the reusability of the acid.

The remaining HNO_3 solution contained silver and lead. To recover the silver, 5 M hydrochloric acid was added to precipitate

silver chloride which was converted into silver oxide using NaOH and reduced to silver powder via hydrazine hydrate. The silver powder was melted into a bar with a recovery of 99.7 wt%.^[48] The silver was electrolytically purified by being used as an anode with a SUS 304 stainless steel cathode. A solution of 0.06 M nitric acid containing 0.3 M AgNO₃ was used as the electrolyte. The final silver recovery achieved for was 90 wt% with a purity of 99.99%.^[48]

Huang et al.^[49] suggested that direct electrowinning is preferable over metallurgical methods, as it is more cost-effective and can sequentially recover multiple metals from the one leaching solution. To demonstrate and examine the variables of applying electrowinning to solar cell metal recovery, a simulated solution was made by mixing metal pellets in the mass ratio of 0.7% silver, 74.4% copper, 12.4% lead, and 12.4% tin. The metals were then dissolved in a 100 mL beaker with 11.4 wt% (\approx 5 M) nitric acid at 60 °C to aid the dissolution then cooled back to 25 °C. The solution was observed to be a blue color due to the presence of Cu²⁺ ions and a white SnO₂ precipitate was formed and recovered by filtration.^[49] A three-electrode system was then used to conduct voltammetry and electrowinning. Titanium and platinum foils were used as the working and counter electrodes respectively with a Ag/AgCl reference. Figure 8 shows the voltammogram obtained by Huang et al.^[49] with a scan rate of 10 mV s⁻¹.

Two reduction peaks are observed. The first peak begins at \approx 0.43 V, reaching maximum at 0.35 V which corresponds to the more noble metal silver, while the second peak occurs at 0.10 V and corresponds with copper reduction. Huang et al.^[49] used the Nernst equation to calculate the theoretical reduction potentials under the used conditions for Ag⁺, Cu²⁺, and Pb²⁺ to be 0.45, 0.13, and -0.38 V, respectively. These values approximated the measured reduction peaks for silver and copper, while the lead reduction peak was masked by that of copper due to the much larger concentration of copper than lead.^[49]

The silver was then extracted at 0.30 V versus Ag/AgCl for 5.6 h. This resulted in a 74.0 wt% recovery with a silver purity of 99.0% and a current efficiency of 99.7%. The copper was extracted next for 24 h at -0.30 V versus Ag/AgCl with a recovery of 83.0 wt% with a 99.0% purity. During the copper recovery, it was also found that the lead ions in solution were deposited at the counter electrode as a nonstoichiometric lead oxide.

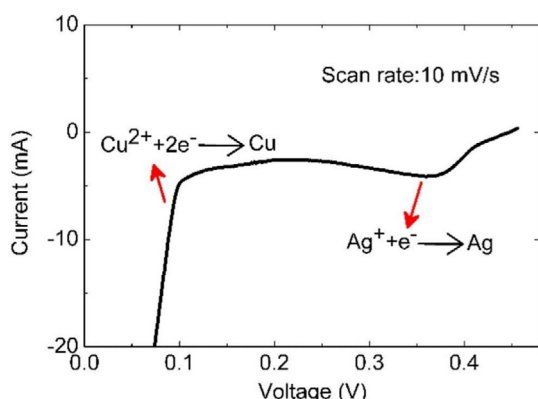


Figure 8. Voltammetry of the leaching solution between 0.5 and 0.0 V versus Ag/AgCl. Reproduced with permission.^[49] Copyright 2017, Elsevier.

Huang et al.^[49] tested the solution via inductively coupled plasma optical emission spectroscopy (ICP-OES) and found that over 99% of the lead ions had been removed from solution, most likely at the counter electrode as a result of oxidation. Additionally, Huang et al.^[49] stated that the recovery of silver and copper was low as deposits came off the electrodes during transfer and rinsing before the deposited mass was weighed. Other observations made were that the pH is an important variable and if it is too low then the deposits can be redissolved into solution, and lower-cost electrode materials should be investigated.^[49]

Deng et al.^[50] developed a novel electrochemical method to simultaneously leach and recover silver. This process uses a whole solar cell as the anode, a silver coil cathode, and a dilute electrolyte containing 5.0 g L⁻¹ silver mostly in the form of AgNO₃. The applied current would oxidize the silver at the surface of the solar cell anode which is then deposited and collected at the cathode. This process is described as having accelerated leaching kinetics when compared to traditional acid leaching due to electrochemically driven oxidation.^[50] However, there are engineering challenges to elevate this process to a larger scale to make it industrially competitive with traditional acid leaching. Significantly, it was observed that lower current densities (<22 mA cm⁻²) improve the efficiency of the process and recommended an optimal current density between 3 and 11 mA cm⁻². This is due to higher current densities leading to dendritic silver growth which is susceptible to rapid redissolution, whereas the recommended lower current densities result in a stable granular silver deposit.^[50]

Nitric acid is a commonly used leachate in the literature to extract the metals from recovered solar cells. However, its use can generate large amounts of harmful nitrogen oxides and be consumed in the process.^[51] Modrzynski et al.^[51] investigated an alternative approach which utilized boron-doped diamond (BDD) electrodes in an electrochemically assisted leaching process and metal recovery in a sulfuric acid-based electrolyte. These electrodes have previously been used to generate strong oxidizers to degrade organic pollutants in wastewater treatment.^[51] The BDD electrodes were used to generate peroxydisulfate ions (S₂O₈²⁻) to act as a redox-mediator to dissolve and recover the metals, as shown in Figure 9.^[51]

It was observed that a higher current lead to an increase in peroxydisulfate which resulted in faster metal dissolution, while increasing the sulfuric acid concentration did not improve the dissolution.^[51] Electrochemical analysis was conducted on solutions of 5 M sulfuric acid containing either 0.01 M of silver, copper or tin using a BDD anode, platinum counter electrode,

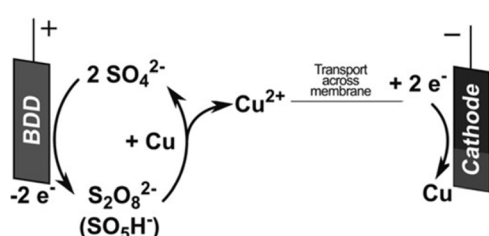


Figure 9. Concept of the electrochemically assisted leaching with sulfuric acid as a cyclical process for metal extraction. Reproduced with permission.^[51] Copyright 2021, John Wiley and Sons.

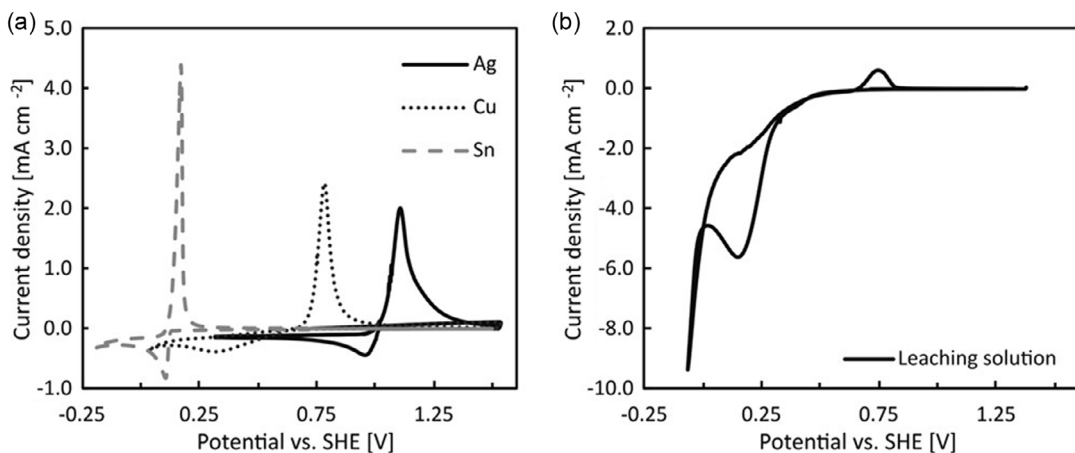


Figure 10. a) Cyclic voltammograms in 5 M H_2SO_4 of 0.01 M solutions of silver, copper, and tin. b) Cyclic voltammogram of a solution obtained by electrochemically etching busbars from a photovoltaic module. Reproduced with permission.^[52] Copyright 2021, John Wiley and Sons.

and a Hg/HgSO_4 reference. The result of which is presented in Figure 10a.^[51]

The comparison in Figure 10a shows the reduction peaks of silver, copper, and tin at 0.97, 0.11, and 0.35 V versus standard hydrogen electrode (SHE), respectively. It also shows that the peaks are well separated by potential similarly to the silver and copper peaks observed in Figure 8, showing the possibility of sequential electrowinning. However, there appears to be an imbalance between the reduction and the larger oxidation peaks (as the oxidation charge is greater than the reduction charge), indicating side reactions in addition to the reoxidation of the metals. This could be the oxidation of the working electrode material or electrolyte oxidation. Figure 10b shows analysis conducted on a solution which was used to electrochemically dissolve a photovoltaic busbar recovered from a module. In contrast to Figure 10a,b presents a copper reduction peak at ≈ 0.40 V versus SHE as well as a strong “reduction wave” of peroxydisulfate. Thus, the tin reduction peak is masked due to the more concentrated peroxydisulfate, while the copper oxidation peak is visible at 0.80 V versus SHE. Electrowinning was conducted with BDD anodes (2.5 cm^2) and glass carbon plate cathodes (8 cm^2). These experiments showed that copper recovery reached close to 100 wt% in 2 h with a current efficiency of almost 100% and was limited by mass transport. Additionally, peroxydisulfate concentrations above 0.1 M would reduce at the cathode in competition with copper reduction as well as the reoxidation of deposited copper. The silver recovery was unaffected by the presence of the peroxydisulfate with ≈ 80 wt% of the silver recovered in the first half hour, with a current efficiency of 20% due to the low silver concentration.^[51] For tin, no recovery was achieved in the presence of peroxydisulfate even when enough charge was applied to completely reduce it into sulfate. It was theorized that this is due to the oxidation of $\text{Sn}(\text{II})$ to $\text{Sn}(\text{IV})$ which can precipitate as a dispersed complex of SnO_2 .^[51]

6. Silicon Purification

The current dominant method for turning metallurgical-grade silicon with a purity between 98% and 99% into solar-grade

silicon is the Siemens process, accounting for $\approx 90\%$ of global polysilicon production.^[52] This process utilizes a fluidized bed reactor at 300 to 350 °C and between 1 and 5 bar pressure to react the metallurgical silicon with hydrogen and hydrogen chloride to generate chlorosilanes. The exit gas is then fractionally separated to remove excess hydrogen and hydrogen chloride from the condensed chlorosilanes.^[52] Distillation is employed to separate a 99.99% trichlorosilane stream from the other chlorosilane byproducts such as silicon tetrachloride.^[52b] The trichlorosilane stream then undergoes chemical vapor deposition in a Siemens reactor onto a U-shaped silicon seed bar electrically heated to 1,100 °C. This results in the growth of large rods of high-purity solar-grade polysilicon silicon (99.999%).^[5,52]

This process is highly energy intensive and can consume up to 160 kWh kg⁻¹ of polysilicon, which correlates to approximately half the embodied energy of a solar module.^[52b,53] Additionally, Table 2 shows a comparison of the typical chemical analysis of metallurgical and solar-grade silicon.^[54] This shows the

Table 2. Typical chemical analysis of metallurgical and solar-grade silicon.^[55]

Element	Metallurgical-grade silicon [ppm]	Solar-grade silicon [ppm]
Si ^{a)}	99%	99.9999%
Fe	2,000–3,000	<0.3
Al	1,500–4,000	<0.1
Ca	500–600	<0.1
B	40–80	<0.3
P	20–50	<0.1
C	600	<3
O	3,000	<10
Ti	160–200	<0.01
Cr	50–200	<0.1

^{a)}Si content in mass %.

requirements of solar-grade silicon and also sets a benchmark for recycled silicon to compete against raw material production.

In terms of solar panel recycling, once the metals have been removed and recovered the remaining valuable component is silicon. This was the motivation for the works of Klugmann-Radziemska et al.^[19] Kang et al.^[41] and Riech et al.^[42] to utilize harsh chemicals such as hydrofluoric acid to etch away contaminated wafer layers (e.g., antireflective coating and n-p junction) to recover high-purity solar-grade silicon.

Alternatively, high-temperature electrorefining of metallurgical-grade silicon to solar-grade silicon has been explored in the literature^[55] and could be applied to recycled silicon. As a result, this process could negate the use of hydrofluoric acid and could produce highly pure silicon for upgraded applications. It has been previously shown that high-temperature silicon electrorefining can produce a silicon product with 99.999% purity with an embodied energy $\approx 12 \text{ kWh kg}^{-1}$.^[53] Figure 11 shows the general electrochemical cell configuration used in literature to refine the contaminated silicon from the anode to the cathode, with contaminants remaining in the electrolyte. Different electrode configurations have been explored in the literature and these have been summarized schematically in Figure 11. Configuration (1) is a solid anode and solid cathode used by Kongstein et al.^[53] (2) is an approach using a copper-based liquid alloy anode and solid cathode used by Cai et al.^[56] and (3) uses a copper-based liquid alloy anode and an aluminum-based liquid alloy cathode as explored by Oishi et al.^[55]

Electrode configuration (1) in Figure 11 was explored mostly by Kongstein et al.^[53] through the use of a metallurgical-grade silicon anode and either tungsten or molybdenum cathodes, in a calcium chloride-based electrolyte. Sodium chloride and calcium oxide were added to the electrolyte to increase ionic conductivity and silicon solubility respectively. Electrochemical analysis was conducted and showed that the reduction peaks for silicon ($-0.2 \text{ V vs silicon}$) and calcium ($-1.0 \text{ V vs silicon}$) were well separated, showing the possibility of selective silicon deposition from the calcium chloride-based melt.^[53] Further investigations showed that the silicon had a fast dissolution

in the melt, reaching equilibrium after 20 min. Electrorefining was conducted at 850°C and it was observed that the contaminated silicon anode would passivate, and the cell potential would reach the overload potential of 30 V when left to run overnight. The anode passivation was due to the formation of silica on the surface of the silicon anode creating an insulative layer and increasing electrical resistance.^[53] To combat anode passivation the current was pulsed at 1 Hz, allowing for a deposition time of 24 h before passivation. While Kongstein et al.^[53] was able to successfully deposit silicon on the working electrode, they highlight the problematic nature of anode passivation being the major barrier. Preliminary electrorefining experiments were also conducted by Cai et al.^[56] in a similar melt composition at 950°C with a solid metallurgical-grade silicon anode (configuration (1) in Figure 11). These experiments were unsuccessful due to anode passivation similar to Kongstein et al.^[53]

To combat anode passivation, liquid alloy anodes were investigated by Cai et al.^[56] as seen as electrode configuration (2) in Figure 11. Cai et al.^[56] utilized a 31 wt% silicon and 69 wt% copper alloy which was liquid at the operating temperature. It was highlighted that the liquid anode could segregate impurities by retaining elements more noble than silicon (e.g., boron and phosphorous) in the anode. Other than the anode, experimental conditions used by Cai et al.^[56] were similar to that of Kongstein et al.^[54] in terms of melt composition, tungsten cathode, temperature range between 700 and 950°C , and under an argon atmosphere. Initially, tungsten electrodes were used to investigate the electrochemistry of the silicon in the melt through cyclic voltammetry which can be seen in Figure 12.^[56]

Observed in Figure 12a is an increased cathodic current after silicon deposition ($-0.8 \text{ V vs tungsten}$) due to calcium deposition. Comparing the result obtained by Cai et al.^[56] in Figure 12a to results obtained by Kongstein et al.^[53] reveals differences in observed oxidation/reduction peaks and peak placements. This is mostly due to presence and absence of silicon in the melt, reinforcing the well-separated silicon and calcium peaks and the impact of silicon in the electrolyte. However, comparing Figure 12b^[56] to the results of Kongstein et al.^[53] shows agreement in terms of consistent shape and peak positions. Moreover, Cai et al.^[56] notes that the mobile silicon species in the electrolyte is Si(IV) complexes, and suspected the cathode process to be controlled by the diffusion of these species but was unable to confirm this.

The Si–Cu liquid alloy anode was used by Cai et al.^[56] in potentiostatic electrorefining at -0.75 V versus tungsten for 20 h. The liquid alloy anode was not passivated unlike results obtained with electrode configuration (1), and the current density remained stable between 10 and 80 mA cm^{-2} . The resultant product was observed to be “powdery” and analyzed using inductively coupled plasma atomic emission spectroscopy. It was found that boron and phosphorous content were reduced by 87% and 89%, respectively, but still above the requirements for solar-grade silicon outlined in Table 2. However, the copper content increased by over ten times the original amount and was suspected to be a result of copper codeposition from the electrolyte. The current efficiency was estimated to be 31% and was thought to be lower than expected due to the low yield as the deposited silicon would break off the cathode in the melt. Cai et al.^[56] states that the issues around the copper content and low yield can be solved by

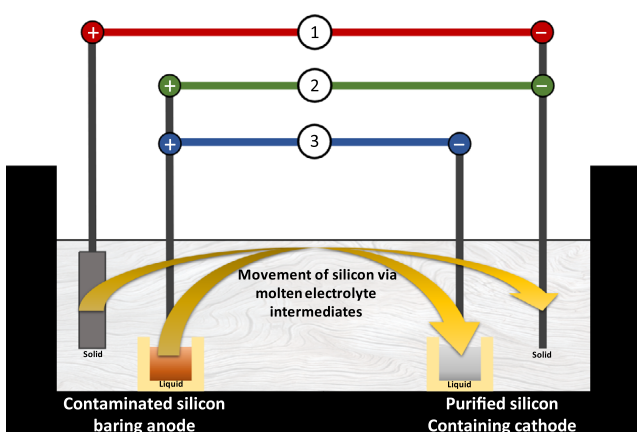


Figure 11. Comparison of high-temperature electrochemical cell configurations used in literature for metallurgical silicon electrorefining; (1) solid anode—solid cathode,^[53] (2) liquid alloy anode—solid cathode,^[56] and (3) liquid alloy anode—liquid alloy cathode.^[55]

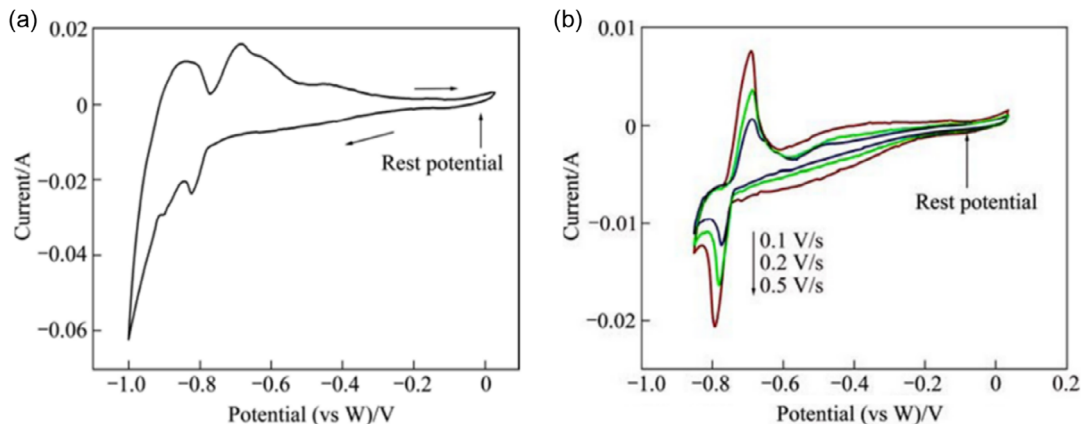


Figure 12. Cyclic voltammograms in molten 85 mol% CaCl_2 , 5 mol% NaCl , 5 mol% CaO , and 5 mol% Si at 850 °C with tungsten electrodes of a) single sweep with scan rate of 0.5 V s^{-1} from 0.0 V to -1.0 V versus W and b) varying sweep rates of 0.1, 0.2, and 0.5 V s^{-1} from 0.0 to -0.85 V versus W. Reproduced with permission.^[56] Copyright 2012, Elsevier.

improving cell design. The energy consumption was also approximated to 9.3 kWh kg^{-1} of silicon which is significantly lower than the requirement of the Siemens process. Haarberg^[57] also investigated the use of liquid alloy anodes (16.5 wt% Si and 83.5 wt% Cu) under similar conditions and found it effective for removing iron, aluminum, and titanium, while it also reduced boron and phosphorous content to 1 and 5 ppm, respectively. Similar to Cai et al.^[56] this product generated by Haarberg^[57] does not comply with solar-grade silicon requirements and observed an increase in copper content by 18%, which would be expected to originate at the copper-containing anode used for the contaminated silicon. Haarberg^[57] also proposes successive electrolysis steps to increase subsequent silicon purity. As a result, this could be an effective process for upgrading recovered silicon from recycled solar panels which is assumed to have a purity existing between metallurgical and solar grade.

The third electrode configuration explored in literature, configuration (3) in Figure 11, uses liquid electrodes for both the anode and cathode. Oishi et al.^[55] used an Si–Cu alloy anode (17 wt% metallurgical silicon and 83 wt% copper), with a liquid aluminum cathode. To obtain the refined silicon from the liquid aluminum cathode, it was precipitated by slowly cooling the sample inside the reaction chamber. The tests were conducted in a cryolite-based melt (NaF/AlF_3 molar ratio of 2.7 with 1 wt% silica and 9 wt% alumina) at 1,000 °C under argon. During refining, the highest partial cathodic current efficiency was achieved with 500 mA cm^{-2} under galvanostatic electrolysis. The maximum current efficiency reported was $\approx 30\%$, while in agreement with Cai et al.^[56] still lower than expected due to multiple side reactions occurring between the electrode and the melt as well as within the melt itself. The most impactful side reaction in this process was the indirect reduction of silicon in the melt, resulting in the accumulation of silicon in the electrolyte and not in the cathode. Increasing the silica concentration in the electrolyte to 2 wt% showed improvement in the partial cathodic current efficiency. Purified silicon was analyzed via glow discharge mass spectrometry, which showed a high purification effect for iron, vanadium, nickel, manganese, and titanium.^[55]

Unique to Oishi et al.^[55] was the use of this method to refine a silicon feedstock derived from recovered wafers from photovoltaic modules. Similar results were achieved with the recovered silicon as with the metallurgical silicon. However, the point of difference between the metallurgical and recovered silicon was in the contamination content. Key impurities for metallurgical grade are iron, vanadium, nickel, manganese, and titanium. Impurities in recovered silicon are more limited to those intentionally added in panel manufacturing such as silver, aluminum, boron, phosphorous, and sodium.^[55] While individual contaminant concentrations were reduced to less than 10 ppm each, the purification was inconclusive for aluminum, boron, and iron. The aluminum and iron contamination in the product silicon was explained to be from the aluminum cathode (with iron being a significant contaminant in the aluminum used), and the boron contamination coming from the boron nitride crucibles. Oishi et al.^[55] concluded the process is effective in silicon refining, however, more work is required on cell construction, silicon precipitation, and careful attention should be paid to the materials used for electrolysis. Olsen and Rolseth^[58] also investigated electrode configuration (3), however, positioned them as three immiscible layers in order of density (Si–Cu anode at the bottom, $\text{CaF}_2/\text{BaF}_2$ based electrolyte in the middle layer, and the liquid silicon cathode at the top). Thermodynamic analysis showed uncertainties in the relative stability of boron and silicon in a fluoride-based melt, inferring codeposition. This was also shown experimentally at 1,500 °C under argon, while other elements showed decent removal when compared to the anode, with a cathodic current efficiency of 97% achieved. Olsen and Rolseth^[58] concluded that the key challenge to metallurgical-grade silicon electrorefining is boron removal, and the production of solar-grade silicon could be possible if a low-boron feedstock is used (possibly recovered silicon from recycled modules).

Research emphasis has been placed on the electrodes, typically the anode, and how it affects the electrorefining process. However, the electrolyte is also important to the process as it facilitates the electrochemical reaction and influences the electrochemistry of the cell. Calcium chloride-based melts have been explored due to their utility at relatively low temperatures

(<1,000 °C), with additions of sodium chloride and calcium oxide to increase electrical conductivity and silicon solubility.^[53,56,57] Other works utilized fluoride-based melts at much higher temperatures (>1,000 °C).^[55,58] It is currently unclear the differences that chloride or fluoride-based electrolytes can have on silicon purity with further investigations necessary.

Table 3 summarizes the operating conditions investigated in the literature to date to highlight the differences and similarities discussed.

The electrolyte has a substantial impact on the overall electro-refining process and as a result, impurities in the electrolyte can affect the final purity of the product silicon. Tseng et al.^[59] investigated electrolyte purification with the idea that it could be used periodically to remove impurities introduced into the melt as a result of silicon electrorefining. Essentially, this work aimed to investigate the feasibility of reusing the molten salt electrolyte in upgrading metallurgical silicon to solar-grade silicon. The electrolyte used was a combination of both chloride and fluoride salts (86.2 wt% calcium chloride and 13.8 wt% calcium fluoride) at 900 °C under argon. A platinum wire was used as a pseudo reference and a tungsten wire was used for the working electrode. For salt purification glassy carbon was used as the counter electrode, and for silicon refining metallurgical silicon was used instead. The salt was initially purified at -1.75 V versus platinum for four 6 h blocks, a voltage selected after initial cyclic voltammograms. Subsequent cyclic voltammograms show the eventual disappearance of the reduction peaks.^[59] At the end of the purification process, the current density had decreased from 9.5 to 5.0 mA cm⁻² representing a decrease in impurities in the melt which had been deposited onto the carbon cathode. A silicon anode was then refined in the purified melt at -1.0 V versus platinum to reintroduce impurities expected from a

refining process. The most effective method tested to repurify the contaminated melt was a multipotential purification process as observed in **Figure 13**.^[59]

As seen in **Figure 13a**, the multipotential purification process consisted of the potential holds -1.00 V for 12 h, -1.25 V for 6 h, -1.50 V for 6 h, and -1.75 V versus platinum for 12 h. The increasingly negative potential was used to follow the negative shift of the cyclic voltammogram as the impurities were removed. Additionally, **Figure 13b** compares the regenerated salt after the multipotential refining process to the initial freshly purified salt. It can be seen in **Figure 13b** that the regenerated salt and the initial purified salt exhibit similar electrochemical activity indicating they have the same approximate impurity composition. This shows the salt has been effectively regenerated and can be reused.^[59] However, Tseng et al. did not report the effect of salt purification on the grade of silicon deposited. Boron concentrations in the electrolyte before and after purification were also not reported which Olsen and Roth^[58] identified as a key issue for electrorefining solar-grade silicon. Moreover, purification of an electrolyte after electropurification of recovered silicon from solar modules would be different to that of metallurgical silicon as the contaminants are vastly different as outlined by Oishi et al.^[55]

Of the reviewed papers, a priority has been placed on the electrode configuration with considerations to the electrolyte and electrochemistry of the system. Major gaps identified are associated with cell design and selection of materials that do not impact on the final silicon purity, how different electrolyte salts and concentrations impact the electrochemistry of the system and contaminants such as boron, and the potential of applying the method to recover silicon from recycled photovoltaic modules as a feedstock for the process.

Table 3. Comparison of the silicon electrorefining conditions investigated in the literature.

Reference	Anode	Cathode	Electrolyte	Temperature	Purity and major contaminants
[53]	Metallurgical-grade silicon	Tungsten or molybdenum wire	81 mol% CaCl 5 mol% NaCl 10 mol% CaO 4 mol% Si	850 °C	35.6 wt% Si 63.0 wt% Mo By EDS analysis
[56]	31 wt% metallurgical-grade silicon 69 wt% copper	Tungsten wire	85 mol% CaCl 5 mol% NaCl 5 mol% CaO 5 mol% Si	700–950 °C	99.98% Si 89.5 ppm Cu 21.4 ppm Fe 19.7 ppm Al By ICP-AES
[57]	16.5 wt% metallurgical-grade silicon 83.3 wt% copper	Carbon rod	60 mol% CaCl 32 mol% NaCl 5 mol% CaO 3 mol% SiO ₂	800–950 °C	Not reported
[55]	17 wt% metallurgical-grade silicon 83 wt% copper	Liquid aluminum	NaF/AlF ₃ (molar ratio 2.7) 1 wt% silica 9 wt% alumina	1,000 °C	99.92% Si 500 ppm Al 300 ppm B By GD-MS
[58]	Liquid silicon copper alloy anode	Liquid silicon	CaF ₂ /BaF ₂	1,500 °C	99.79% Si 1,500 ppm Al 550 ppm Cu By GD-MS

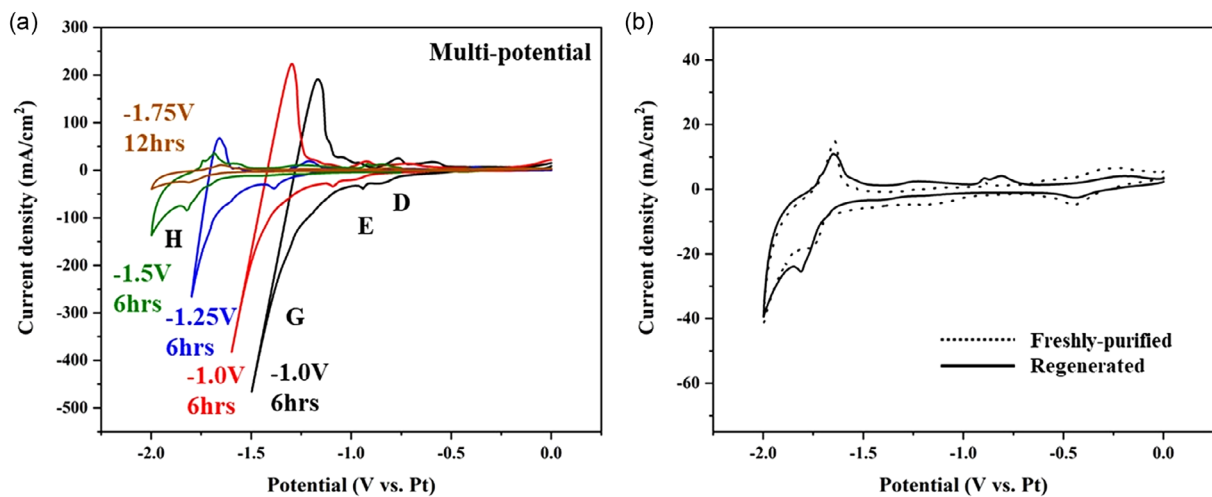


Figure 13. Cyclic voltammetry a) after each step of multipotential purification and b) of freshly purified salt as compared to regenerated salt. Reproduced with permission.^[59] Copyright 2021, Elsevier.

7. Electrochemical-Based Solar Module Recycling Process

Figure 14 proposes an electrochemical-based solar module recycling process by bringing together the reviewed literature; disassembly of the frame and junction box, delamination of glass, encapsulant, and backsheet, extraction of metals from the photovoltaic cells via chemical leaching and electrowinning, and upgrading of recovered silicon through electrorefining.

While the literature has been focused on investigating the execution of individual unit operations, very little consideration has been given to the balance of system. This would importantly look at how the product from one unit operation becomes the feedstock for the next, fulfilling the requirements and allowable tolerances and degree of separations. While disassembly has

been well established, there is still consideration around effective delamination on an industrial level. Chemical leaching of photovoltaic cell materials has been investigated along the metallurgical route, but very little attention has been given to the process being upstream of delamination. Additionally, electrowinning of metals leached from recovered photovoltaic cells is currently a gap in the process, with most of the research centered on feasibility and simulated solutions. Moreover, electrorefining of silicon is still undergoing development and has not yet been able to produce solar-grade silicon. The potential of using electrorefining to upgrade recycled silicon has not yet been comprehensively explored. Furthermore, the limitations of this process with regards to metallurgical silicon might become obsolete when applied to recovered silicon, representing an exciting new opportunity for a circular economy approach to renewable energy.

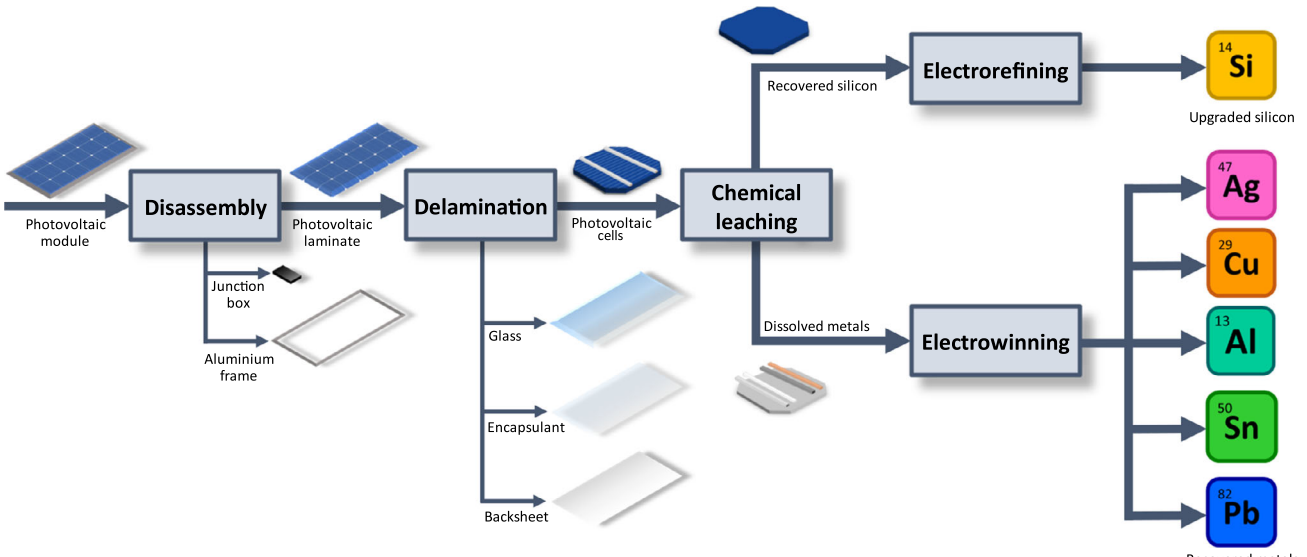


Figure 14. Diagrammatic representation of an electrochemical-based solar module recycling process.

8. Conclusion

There is currently no commercial solar panel recycling process on an industrial level with the comprehensive recovery of the majority of materials in an energy and environmentally conscious manner. This is due to the barriers identified here, that must be engineered around; effective module delamination, liberation of silicon and metals from plastics while minimizing energy usage and pollution generation, and the output requirements of delamination and liberation for upstream materials extraction processes. Therefore, it is crucial to understand the recycling process from a holistic view and understand how operational outputs influence upstream systems.

The upstream extraction processes have been primarily explored through hydrometallurgical methods, which require the use of multiple harsh chemicals and separation processes. As discussed here, electrochemical methods could streamline recovery through direct selective electrowinning from a single leachate solution. Although initial research shows the feasibility of electrochemical recovery with simulated solutions, there is limited exploration of this technology using a recovered solar cell feedstock. More notably there is a necessity to understand how delamination methods impact chemical leaching for electrowinning and highlighted here the extent of delamination required for effective recovery. Moreover, additional research is required into electrode materials, temperature, alternative electrochemical leaching methods, and overall process electrochemistry. This analysis could help develop the process beyond laboratory scale to allow for the feasibility of a cost-effective pilot process.

Subsequently, it is proposed here that recovered silicon upgrading should be included in the solar module recycling process to create a truly circular process. High-temperature electro-refining is yet to successfully upgrade metallurgical-grade silicon to solar-grade quality but could be potentially used to treat recovered silicon from recycled modules. The process limitations include design and materials, optimal electrode configuration, and melt electrochemistry for impurity segregation. However, these limitations could prove to be advantageous if the feed material is changed from metallurgical-grade silicon to recovered silicon from recycled modules due to the different contaminants impacting the chemistry of refining.

Overcoming these technological and process limitations is essential to advancing solar panel recycling and achieving sustainability in the renewable energy sector. By developing scalable, efficient recycling methods EOL solar modules can be transformed from a waste stream to a valuable resource, fostering a resilient circular economy that supports the global transition to clean energy.

Supporting Information

Supporting Information is available from the Wiley Online Library or from the author.

Acknowledgements

This work was made possible because of funding from the CSIRO Industry PhD program. The CSIRO Industry PhD Program is part of an Australian

Government initiative to better translate university research into commercial outcomes. This work would also like to acknowledge contributions and support from James Petesc and Tom Witheridge at PV Industries and scholarship funding from PV Industries.

Conflict of Interest

The authors declare no conflict of interest.

Author Contributions

Jackson Lee: data curation (lead); formal analysis (lead); investigation (lead); methodology (lead); visualization (lead); writing—original draft (lead); writing—review and editing (supporting). **Noel Duffy:** conceptualization (equal); funding acquisition (lead); project administration (equal); supervision (supporting); writing—review and editing (supporting). **Jessica Allen:** conceptualization (equal); funding acquisition (supporting); methodology (supporting); project administration (equal); supervision (lead); visualization (supporting); writing—review and editing (equal).

Keywords

circular economy, electrochemical, electrorefining, photovoltaics, recycling

Received: August 18, 2024

Revised: November 15, 2024

Published online: December 12, 2024

- [1] H. X. Li, D. J. Edwards, M. R. Hosseini, G. P. Costin, *J. Cleaner Prod.* **2020**, 242, 118475.
- [2] R. Newell, D. Raimi, S. Villanueva, B. Prest, *Resour. Future* **2020**, https://media.rfi.org/documents/GEO_2020_Report.pdf.
- [3] C. Breyer, D. Bogdanov, A. Gulagi, A. Aghahosseini, L. S. N. S. Barbosa, O. Koskinen, M. Barasa, U. Caldera, S. Afanasyeva, M. Child, J. Farfan, P. Vainikka, *Prog. Photovoltaics: Res. Appl.* **2017**, 25, 727.
- [4] a) I. D'Adamo, F. Ferella, M. Gastaldi, N. M. Ippolito, P. Rosa, *Waste Manage. Res.* **2023**, 41, 1144; b) IRENA and IEA-PVPS, International Renewable Energy Agency and International Energy Agency Photovoltaic Power Systems **2016**, ISBN: 978-92-95111-99-8. c) IEA-PVPS, Snapshot of Global PV Markets **2024**, <https://doi.org/10.69766/VHFR4040>, ISBN: 978-3-907281-55-0.
- [5] G. A. Heath, T. J. Silverman, M. Kempe, M. Deceglie, D. Ravikumar, T. Remo, H. Cui, P. Sinha, C. Libby, S. Shaw, K. Komoto, K. Wambach, E. Butler, T. Barnes, A. Wade, *Nat. Energy* **2020**, 5, 502.
- [6] N. F. Hengky Salim, Benjamin Madden, *Inst. Sustainable Futures, Univ. Technol. Sydney* **2023**, https://www.uts.edu.au/sites/default/files/2023-06/2.%20Key%20Findings%20from%20Installer%20Survey_0.pdf.
- [7] M. K. H. Rabaia, C. Semeraro, A.-G. Olabi, *J. Cleaner Prod.* **2022**, 373, 133864.
- [8] A. Divya, T. Adish, P. Kaustubh, P. S. Zade, *Sol. Energy Mater. Sol. Cells* **2023**, 253, 112151.
- [9] a) M. de Wild-Scholten, E. Alsema, *Refocus* **2004**, 5, 46; b) G. Yıldız, B. Çalış, A. E. Gürel, İ. Ceylan, *Environ. Nanotechnol. Monit. Manage.* **2020**, 14, 100343.
- [10] a) A. Sharma, S. Pandey, M. Kolhe, *Int. J. Smart Grid Clean Energy* **2019**, 8, 597; b) J. Ylä-Mella, K. Poikela, U. Lehtinen, P. Tanskanen, E. Román, R. L. Keiski, E. Pongrácz, *J. Waste Manage.* **2014**, 2014.

- [11] A. Levin, B. Dixon, Environmental Law and Policy Monitor, **2020**, <https://www.environmentallawandpolicy.com/2020/10/california-classifies-solar-panels-as-universal-waste/>.
- [12] DCCEEW, Wired for Change: Regulation for small electrical products and solar photovoltaic systems wast, Canberra **2023**, <https://consult.dcceew.gov.au/regulation-small-electrical-products-solar-pv>.
- [13] a) M. Akhter, A. Al Mansur, M. I. Islam, M. S. H. Lipu, T. F. Karim, M. G. M. Abdolrasol, T. A. H. Alghamdi, *Sustainability* **2024** *16*, 5785; b) IEA-PVPS, **2024**.
- [14] M. H. Shubbak, *Renewable Sustainable Energy Rev.* **2019**, *115*, 109383.
- [15] a) D. Strachala, J. Hybský, J. Vaněk, G. Fafilek, K. Jandová, *Acta Montan. Slovaca* **2017**, *22*; b) X. Wang, X. Tian, X. Chen, L. Ren, C. Geng, *Sol. Energy Mater. Sol. Cells* **2022**, *248*, 111976.
- [16] DuPont, (Ed: DuPont), DuPont, **2016**.
- [17] K. J. Geretschläger, G. M. Wallner, J. Fischer, *Sol. Energy Mater. Sol. Cells* **2016**, *144*, 451.
- [18] R. Deng, N. L. Chang, Z. Ouyang, C. M. Chong, *Renewable Sustainable Energy Rev.* **2019**, *109*, 532.
- [19] E. Klugmann-Radziemska, P. Ostrowski, *Renewable Energy* **2010**, *35*, 1751.
- [20] a) W.-S. Chen, Y.-J. Chen, K.-C. Yueh, C.-P. Cheng, T.-C. Chang, *IOP Conf. Ser.: Mater. Sci. Eng.* **2020**, *720*, 012007; b) R. Deng, Y. Zhuo, Y. Shen, *Resour. Conserv. Recycl.* **2022**, *187*, 106612; c) P. Dias, L. Schmidt, M. Monteiro Lunardi, N. L. Chang, G. Spier, R. Corkish, H. Veit, *Resour. Conserv. Recycl.* **2021**, *165*, 105241; d) V. Fiandra, L. Sannino, C. Andreozzi, G. Graditi, *Waste Manage.* **2019**, *84*, 91; e) R. Gahlot, S. Mir, N. Dhawan, *Energy Fuels* **2022**, *36*, 14554; f) G. Granata, P. Altimari, F. Pagnanelli, J. De Greef, *J. Cleaner Prod.* **2022**, *363*, 132384; g) C. E. L. Latunussa, F. Ardente, G. A. Blengini, L. Mancini, *Sol. Energy Mater. Sol. Cells* **2016**, *156*, 101; h) M. S. W. Lim, D. He, J. S. M. Tiong, S. Hanson, T. C.-K. Yang, T. J. Tiong, G.-T. Pan, S. Chong, *J. Cleaner Prod.* **2022**, *340*, 130796; i) M. Tao, V. Fthenakis, B. Ebin, B.-M. Steenari, E. Butler, P. Sinha, R. Corkish, K. Wambach, E. S. Simon, *Prog. Photovoltaics: Res. Appl.* **2020**, *28*, 1077.
- [21] P. K. Enaganti, A. Bhattacharjee, A. Ghosh, Y. N. Chanchangi, C. Chakraborty, T. K. Mallick, S. Goel, *Energy* **2022**, *239*, 122213.
- [22] a) H. Sverdrup, D. Koca, K. V. Ragnarsdottir, *Resour. Conserv. Recycl.* **2014**, *83*, 121; b) S. Northey, S. Mohr, G. M. Mudd, Z. Weng, D. Giurco, *Resour. Conserv. Recycl.* **2014**, *83*, 190.
- [23] N. Rötzer, M. Schmidt, *Resources* **2020**, *9*, 44.
- [24] V. Muteri, M. Cellura, D. Curto, V. Franzitta, S. Longo, M. Mistretta, M. L. Parisi, *Energies* **2020**, *13*, 252.
- [25] H. F. Yu, M. Hasanuzzaman, N. A. Rahim, N. Amin, N. Nor Adzman, *Sustainability* **2022**, *14*, 8567.
- [26] P. Nain, A. Kumar, *Waste Manag.* **2020**, *114*, 351.
- [27] R. Vinayagamoorthi, P. B. Bhargav, N. Ahmed, C. Balaji, K. Aravindh, A. Krishnan, R. Govindaraj, P. Ramasamy, *J. Environ. Chem. Eng.* **2024**, *12*, 111715.
- [28] P. Dias, L. Schmidt, L. B. Gomes, A. Bettanin, H. Veit, A. M. Bernardes, *J. Sustainable Metall.* **2018**, *4*, 176.
- [29] R. A. de Souza, H. M. Veit, *Circ. Econ.* **2023**, *2*, 100027.
- [30] R. Frischknecht, K. Komoto, T. Doi, **2023**, ISBN: 978-3-907281-41-3.
- [31] V. Fiandra, L. Sannino, C. Andreozzi, F. Corcelli, G. Graditi, *Waste Manag.* **2019**, *87*, 97.
- [32] a) D. M. Abdo, T. Mangialardi, F. Medici, L. Piga, *Processes* **2023**, *11*, 1848; b) D. Sah, P. Saini, S. Kumar, *Sol. Energy* **2022** *31*.
- [33] R. Wang, E. Song, C. Zhang, X. Zhuang, E. Ma, J. Bai, W. Yuan, J. Wang, *RSC Adv.* **2019**, *9*, 18115.
- [34] M. S. Chowdhury, K. S. Rahman, T. Chowdhury, N. Nuthammachot, K. Techato, M. Akhtaruzzaman, S. K. Tiong, K. Sopian, N. Amin, *Energy Strategy Rev.* **2020**, *27*, 100431.
- [35] T. Doi, I. Tsuda, H. Unagida, A. Murata, K. Sakuta, K. Kurokawa, *Sol. Energy Mater. Sol. Cells* **2001**, *67*, 397.
- [36] G. H. Brenes, I. Riech, G. Giácoman-Vallejos, A. González-Sánchez, V. Rejón, *Sol. Energy* **2023**, *263*, 111778.
- [37] J. Lee, N. Duffy, J. Petesic, T. Witheridge, J. Allen, *Waste Manage.* **2024**, *190*, 122.
- [38] E. Bellini, *Pv magazine* **2022**. <https://www.pv-magazine.com/2022/10/24/new-industrial-plant-concept-for-end-of-life-pv-panel-recycling/>.
- [39] S. P. Gundupalli, S. Hait, A. Thakur, *Waste manage.* **2017**, *60*, 56.
- [40] Y. Akimoto, A. Iizuka, E. Shibata, *Miner. Eng.* **2018**, *125*, 1.
- [41] N. Dhawan, S. Agrawal, *Min. Metall. Explor.* **2022**, *39*, 2539.
- [42] S. Kang, S. Yoo, J. Lee, B. Boo, H. Ryu, *Renewable Energy* **2012**, *47*, 152.
- [43] I. Riech, C. Castro-Montalvo, L. Wittersheim, G. Giácoman-Vallejos, A. González-Sánchez, C. Gamboa-Loira, M. Acosta, J. Méndez-Gamboa, *Materials* **2021**, *14*, 581.
- [44] D. S. Prasad, B. Sanjana, D. Sai Kiran, P. P. Srinivasa Kumar, R. Ratheesh, *Sustainable Mater. Technol.* **2023**, *37*, e00671.
- [45] Y. K. Yi, H. S. Kim, T. Tran, S. K. Hong, M. J. Kim, *J. Air Waste Manage. Assoc.* **2014**, *64*, 797.
- [46] M. Theocharis, C. Pavlopoulos, P. Kousi, A. Hatzikioseyan, I. Zarkadas, P. E. Tsakiridis, E. Remoundaki, L. Zoumboulakis, G. Lyberatos, *Waste Biomass Valorization* **2022**, *13*, 4027.
- [47] M. Tao, *ECS J. Solid State Sci. Technol.* **2020**, *9*, 125007.
- [48] T. F. Fuller, J. N. Harb, *Electrochemical Engineering*, John Wiley & Sons, Inc, Hoboken, NJ, USA **2018**.
- [49] B. Jung, J. Park, D. Seo, N. Park, *ACS Sustainable Chem. Eng.* **2016**, *4*, 4079.
- [50] W.-H. Huang, W. J. Shin, L. Wang, W.-C. Sun, M. Tao, *Sol. Energy* **2017**, *144*, 22.
- [51] R. Deng, P. R. Dias, M. M. Lunardi, J. Ji, *Green Chem.* **2021**, *23*, 10157.
- [52] C. Modrzynski, L. Blaesing, S. Hippmann, M. Bertau, J. Z. Bloh, C. Weidlich, *Chem. Ing. Tech.* **2021**, *93*, 1851.
- [53] a) G. Bye, B. Ceccaroli, *Sol. Energy Mater. Sol. Cells* **2014**, *130*, 634; b) C. Ramírez-Márquez, G. Contreras-Zarazúa, M. Martín, J. G. Segovia-Hernández, *ACS Sustainable Chem. Eng.* **2019**, *7*, 5355.
- [54] O. E. Kongstein, C. Wollan, S. Sultana, G. M. Haarberg, *ECS Trans.* **2007**, *3*, 357.
- [55] B. S. Yakalashe, M. Tangstad, *Chem. Technol.* **2012**, *32*, <https://www.911metallurgist.com/wp-content/uploads/2016/02/Silicon-processing-from-quartz-to-crystalline-silicon-solar-cells.pdf>.
- [56] T. Oishi, K. Koyama, M. Tanaka, *J. Electrochem. Soc.* **2016**, *163*, E385.
- [57] J. Cai, X.-T. Luo, C.-H. Lu, G. M. Haarberg, A. Laurent, O. E. Kongstein, S.-L. Wang, *Trans. Nonferrous Met. Soc. China* **2012**, *22*, 3103.
- [58] G. M. Haarberg, presented at *Proc. of the 8 th Pacific Rim Inter. Congress on Advanced Materials and Processing*, **2016**.
- [59] E. Olsen, S. Rolseth, *Metall. Mater. Trans. B* **2010**, *41*, 295.
- [60] M.-F. Tseng, L. Ricci, M. Tao, *Sep. Purif. Technol.* **2021**, *274*, 119030.



Jackson Lee is a Ph.D. candidate in chemical engineering at the University of Newcastle, Australia. Jackson received his B.Eng. (Chem) (Hons) and B.Math. in 2022 at the University of Newcastle. Jackson is a part of the CSIRO Industry PhD program, an Australian Government initiative to better translate university research into commercial outcomes. Working with PV Industries, Jackson's research centers around the recycling of EOL solar modules and the application of electrochemistry to close the gaps in a circular solar economy. This is driven by an interest in energy systems, sustainability, and complex problem solving.



Noel Duffy is a principal research scientist at the CSIRO and the group leader for Solar Technologies. With over 15 years of experience at CSIRO, he is a highly cited author with over 100 publications. Dr. Duffy has been instrumental in the development of various thin-film solar cell technologies, including dye-sensitized solar cells, semiconductor CdTe, CZTS, CIGS, organic photovoltaics (PVs), and more recently, perovskite solar cells. His extensive research interests also encompass the application of electrochemical and photoelectrochemical processes to energy storage devices, solar fuel generation (e.g., hydrogen), and the recycling of critical minerals.



Jessica Allen is currently leading the Electrochemical Engineering Laboratory at the University of Newcastle, Australia, within the Newcastle Institute for Energy and Resources. Dr. Allen is a senior lecturer in chemical engineering with a multidisciplinary background spanning chemistry and engineering and has also spent time in industry as a professional engineer. She is passionate about technology development and science communication and believes both are critical to achieve the level of decarbonization needed to address global climate change.